Viscoplastic fluid flows: applications, simulation strategies and challenges

Jérémy Bleyer
coll.: Mathilde Maillard, Thibaud Chevalier, Philippe Coussot, Xavier Chateau

Laboratoire Navier, ENPC, Univ Gustave Eiffel, CNRS

Fronts
June 26th-27th 2023

Introduction

Viscosity measurements of **clay suspension** in capillaries by **Bingham**

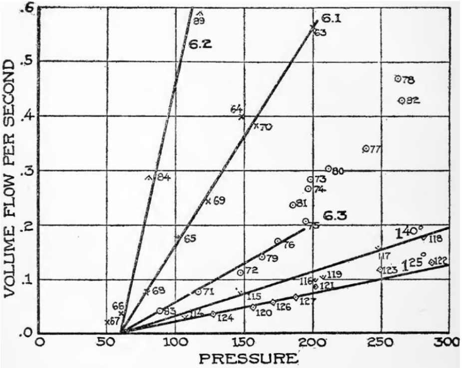

Flow rate (ml/s) vs pressure g/cm^2 for a clay suspension [Bingham, 1916]

Introduction

Viscoplastic fluids = a specific class of **non-Newtonian fluids** with a solid-like behaviour

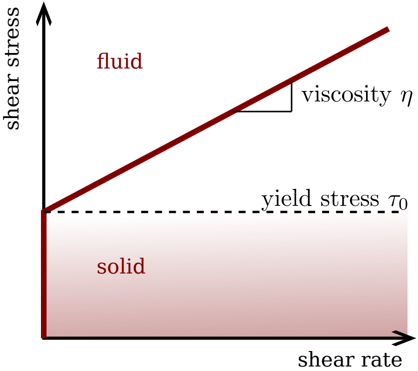

- flow like a simple fluid above a **critical pressure**
- remains at rest, like a solid, below

poses a **challenge** for classification: **solid** or **fluid** ?
radically different than simple **nonlinear viscosity**

Outline

Viscoplastic fluids around us

cosmetics

food

construction, geophysics

Industrial and societal concerns

moving object/coating

spreading/arrest

[Balmforth et al., 2014]

risks

[geologypage.com]

[camp2camp.org]

Viscoplasticity in concrete 3D printing

3d concrete printing at **Laboratoire Navier**, [courtesy Romain Mesnil]

[ ]pc
/F (montage$_3 d_p rinting.mp4)/Postertrue >>, Annotations =<<>>, T =$
$(mmdefaultlabel1), Border =$
$000pdfmark = /PUT, Raw = ThisPage << /AA << /O << /S/Movie/T(mmdefaultlabel$

Challenges for rheologists

- material must be **pumpable** $\tau_0 \approx 1 - 10\text{kPa}$
- material must sustain other layers (**buildability**) $\tau_0 \approx 0.1 - 1\text{MPa}$
- 2 decades of yield stress over 1 hour

fresh state = dense, viscoplastic suspensions
hardened state = brittle, viscoelastic material

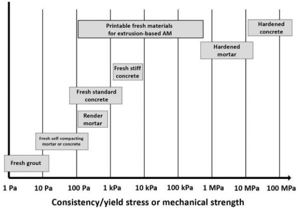

Challenges for rheologists

- material must be **pumpable** $\tau_0 \approx 1 - 10\text{kPa}$
- material must sustain other layers (**buildability**) $\tau_0 \approx 0.1 - 1\text{MPa}$
- 2 decades of yield stress over 1 hour

fresh state = dense, viscoplastic suspensions
hardened state = brittle, viscoelastic material

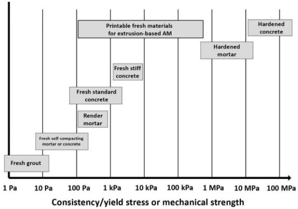

A **low-cost rheometer**: slug test
Mayonnaise drips [Coussot et al, 2005]

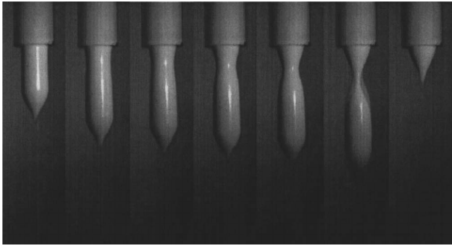

Fresh mortar [Ducoulombier et al., 2021]

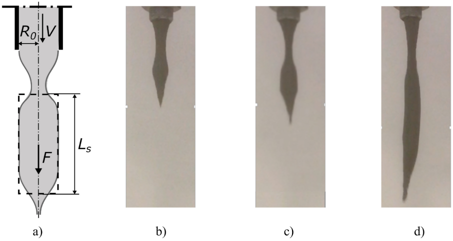

Outline

Variational principle (quasi-statics)

Solution velocity field $\boldsymbol{u}$ obtained from the following minimum principle:

$$
\begin{array}{rl}
(P) = \displaystyle\min_{\boldsymbol{u}} & \displaystyle\int_\Omega \phi(\boldsymbol{d})\,\mathrm{d}\Omega - \mathcal{P}_{\text{ext}}(\boldsymbol{u}) \\
\text{s.t.} & \boldsymbol{d} = \frac{1}{2}(\nabla \boldsymbol{u} + \nabla^{\mathsf{T}} \boldsymbol{u}) \\
& \operatorname{div} \boldsymbol{u} = 0
\end{array}
$$

Akin to minimum potential energy principle in elasticity, dissipation rate principle in GSM

Variational principle (quasi-statics)

Solution velocity field $\boldsymbol{u}$ obtained from the following minimum principle:

$$\begin{array}{rl} (P) = \displaystyle\min_{\boldsymbol{u}} & \displaystyle\int_\Omega \phi(\boldsymbol{d})\,\mathrm{d}\Omega - \mathcal{P}_{\text{ext}}(\boldsymbol{u}) \\ \text{s.t.} & \boldsymbol{d} = \frac{1}{2}(\nabla \boldsymbol{u} + \nabla^{\mathsf{T}} \boldsymbol{u}) \\ & \operatorname{div} \boldsymbol{u} = 0 \end{array}$$

Akin to minimum potential energy principle in elasticity, dissipation rate principle in GSM

Optimality conditions: introduce saddle-point problem

$$\begin{aligned} \max_{\boldsymbol{s},p} \min_{\boldsymbol{u},\boldsymbol{d}} \mathcal{L}(\boldsymbol{u},\boldsymbol{d},\boldsymbol{s},p) &= \max_{\boldsymbol{s},p} \min_{\boldsymbol{u},\boldsymbol{d}} \int_\Omega (\phi(\boldsymbol{d}) - \boldsymbol{s} : (\boldsymbol{d} - \nabla^s \boldsymbol{u}) - p \operatorname{div} \boldsymbol{u})\,\mathrm{d}\Omega - \mathcal{P}_{\text{ext}}(\boldsymbol{u}) \\ &= \max_{\boldsymbol{s},p} \min_{\boldsymbol{u},\boldsymbol{d}} \int_\Omega (\phi(\boldsymbol{d}) - \boldsymbol{s} : \boldsymbol{d})\,\mathrm{d}\Omega - \int_\Omega (\operatorname{div} \boldsymbol{s} - \nabla p) \cdot \boldsymbol{u}\,\mathrm{d}\Omega - \mathcal{P}_{\text{ext}}(\boldsymbol{u}) \end{aligned}$$

Variational principle (quasi-statics)

Solution velocity field $\boldsymbol{u}$ obtained from the following minimum principle:

$$(P) = \min_{\boldsymbol{u}} \quad \int_\Omega \phi(\boldsymbol{d})\,\mathrm{d}\Omega - \mathcal{P}_{\text{ext}}(\boldsymbol{u})$$
$$\text{s.t.} \quad \boldsymbol{d} = \frac{1}{2}(\nabla \boldsymbol{u} + \nabla^{\mathsf{T}} \boldsymbol{u})$$
$$\operatorname{div} \boldsymbol{u} = 0$$

Akin to minimum potential energy principle in elasticity, dissipation rate principle in GSM

Optimality conditions: introduce saddle-point problem

$$\max_{\boldsymbol{s},p} \min_{\boldsymbol{u},\boldsymbol{d}} \mathcal{L}(\boldsymbol{u},\boldsymbol{d},\boldsymbol{s},p) = \max_{\boldsymbol{s},p} \min_{\boldsymbol{u},\boldsymbol{d}} \int_\Omega (\phi(\boldsymbol{d}) - \boldsymbol{s}:(\boldsymbol{d} - \nabla^s \boldsymbol{u}) - p \operatorname{div} \boldsymbol{u})\,\mathrm{d}\Omega - \mathcal{P}_{\text{ext}}(\boldsymbol{u})$$
$$= \max_{\boldsymbol{s},p} \min_{\boldsymbol{u},\boldsymbol{d}} \int_\Omega (\phi(\boldsymbol{d}) - \boldsymbol{s}:\boldsymbol{d})\,\mathrm{d}\Omega - \int_\Omega (\operatorname{div} \boldsymbol{s} - \nabla p)\cdot \boldsymbol{u}\,\mathrm{d}\Omega - \mathcal{P}_{\text{ext}}(\boldsymbol{u})$$

results in:

$$\boldsymbol{s} = \partial_{\boldsymbol{d}} \phi \tag{1}$$
$$\boldsymbol{\sigma} = \boldsymbol{s} - p\boldsymbol{I} \tag{2}$$
$$\operatorname{div} \boldsymbol{\sigma} + \boldsymbol{f} = 0 \tag{3}$$
$$+\,\text{BCs} \tag{4}$$

Some particular behaviours

- **Newtonian** fluid:

$$\phi(\boldsymbol{d}) = \eta \boldsymbol{d} : \boldsymbol{d} \Rightarrow \boldsymbol{\sigma} = 2\eta \boldsymbol{d}$$

Some particular behaviours

- **Newtonian** fluid:

$$\phi(\boldsymbol{d}) = \eta \boldsymbol{d} : \boldsymbol{d} \Rightarrow \boldsymbol{\sigma} = 2\eta \boldsymbol{d}$$

- **Visco-plastic Bingham** fluid:

$$\phi(\boldsymbol{d}) = \eta \boldsymbol{d} : \boldsymbol{d} + \sqrt{2}\tau_0\sqrt{\boldsymbol{d} : \boldsymbol{d}}$$

is **non-smooth**

Some particular behaviours

- **Newtonian** fluid:

$$\phi(\boldsymbol{d}) = \eta \boldsymbol{d} : \boldsymbol{d} \Rightarrow \boldsymbol{\sigma} = 2\eta \boldsymbol{d}$$

- **Visco-plastic Bingham** fluid:

$$\phi(\boldsymbol{d}) = \eta \boldsymbol{d} : \boldsymbol{d} + \sqrt{2}\tau_0 \sqrt{\boldsymbol{d} : \boldsymbol{d}}$$

  is **non-smooth** $\Rightarrow \boldsymbol{\sigma} = \partial_{\boldsymbol{d}}\phi$ should be understood in the sense of **subdifferentials** i.e.:

$$\boldsymbol{\sigma} \in \partial_{\boldsymbol{d}}\phi(\boldsymbol{d}) = \{2\eta \boldsymbol{d}\} + \begin{cases} \boldsymbol{\tau} \in G & \text{if } \boldsymbol{d} = 0 \\ \sqrt{2}\tau_0 \dfrac{\boldsymbol{d}}{\|\boldsymbol{d}\|} & \text{otherwise} \end{cases} \quad \text{where } G = \{\boldsymbol{\tau} \text{ s.t. } \|\boldsymbol{\tau}\| \leq \sqrt{2}\tau_0\}$$

Some particular behaviours

- **Newtonian** fluid:

$$\phi(\boldsymbol{d}) = \eta \boldsymbol{d} : \boldsymbol{d} \Rightarrow \boldsymbol{\sigma} = 2\eta \boldsymbol{d}$$

- **Visco-plastic Bingham** fluid:

$$\phi(\boldsymbol{d}) = \eta \boldsymbol{d} : \boldsymbol{d} + \sqrt{2}\tau_0 \sqrt{\boldsymbol{d} : \boldsymbol{d}}$$

  is **non-smooth** $\Rightarrow \boldsymbol{\sigma} = \partial_{\boldsymbol{d}} \phi$ should be understood in the sense of **subdifferentials** i.e.:

$$\boldsymbol{\sigma} \in \partial_{\boldsymbol{d}}\phi(\boldsymbol{d}) = \{2\eta \boldsymbol{d}\} + \begin{cases} \boldsymbol{\tau} \in G & \text{if } \boldsymbol{d} = 0 \\ \sqrt{2}\tau_0 \dfrac{\boldsymbol{d}}{\|\boldsymbol{d}\|} & \text{otherwise} \end{cases} \quad \text{where } G = \{\boldsymbol{\tau} \text{ s.t. } \|\boldsymbol{\tau}\| \leq \sqrt{2}\tau_0\}$$

- **Visco-plastic Herschel-Bulkley** fluid:

$$\phi(\boldsymbol{d}) = \frac{K}{m+1} 2^{(m+1)/2} \|\boldsymbol{d}\|^{m+1} + \sqrt{2}\tau_0 \sqrt{\boldsymbol{d} : \boldsymbol{d}}$$

$$\boldsymbol{\sigma} = K 2^{(m+1)/2} \boldsymbol{d} \|\boldsymbol{d}\|^{m-1} + \begin{cases} \boldsymbol{\tau} \in G & \text{if } \boldsymbol{d} = 0 \\ \sqrt{2}\tau_0 \dfrac{\boldsymbol{d}}{\|\boldsymbol{d}\|} & \text{otherwise} \end{cases}$$

Some particular behaviours

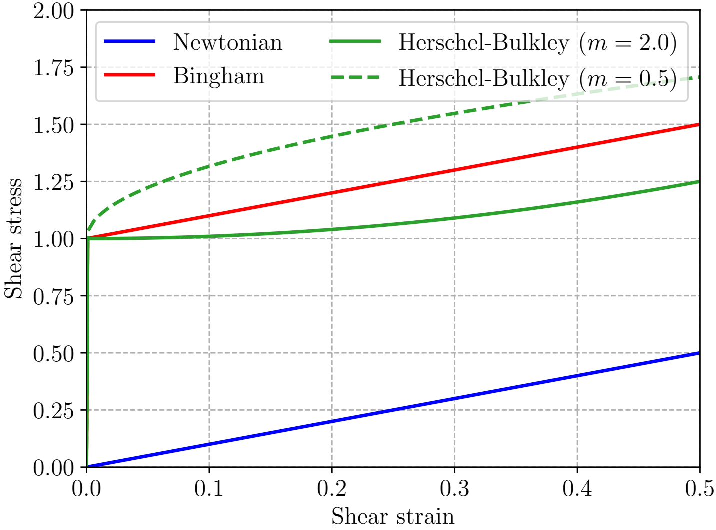

1D behaviour

Generic setting and key features

Generic visco-plastic behaviour: $\phi(\boldsymbol{d}) = \phi_{\text{visc}}(\boldsymbol{d}) + \phi_{\text{plast}}(\boldsymbol{d})$ where:

- **viscous part** ϕ_{visc} is strictly convex (homogeneous of degree $m+1>1$)
- **plastic part** ϕ_{plast} is homogeneous of degree 1. i.e. $\phi^*_{\text{plast}}(\boldsymbol{\sigma}) = \delta_G(\boldsymbol{\sigma})$ is the indicator of a convex set G containing 0

Generic setting and key features

Generic visco-plastic behaviour: $\phi(\boldsymbol{d}) = \phi_{\text{visc}}(\boldsymbol{d}) + \phi_{\text{plast}}(\boldsymbol{d})$ where:

- **viscous part** ϕ_{visc} is strictly convex (homogeneous of degree $m+1>1$)
- **plastic part** ϕ_{plast} is homogeneous of degree 1. i.e. $\phi^*_{\text{plast}}(\boldsymbol{\sigma}) = \delta_G(\boldsymbol{\sigma})$ is the indicator of a convex set G containing 0

Behaviour at small velocities: introduce $\widetilde{\boldsymbol{u}} = \boldsymbol{u}/\epsilon$:

$$\begin{array}{rl} \displaystyle\min_{\widetilde{\boldsymbol{u}}} & \displaystyle\int_\Omega \left(\phi_{\text{visc}}(\epsilon\widetilde{\boldsymbol{d}}) + \phi_{\text{plast}}(\epsilon\widetilde{\boldsymbol{d}})\right)\,\mathrm{d}\Omega - \int_\Omega \boldsymbol{f}\cdot\epsilon\widetilde{\boldsymbol{u}}\,\mathrm{d}\Omega \\ \text{s.t.} & \epsilon\widetilde{\boldsymbol{d}} = \epsilon\frac{1}{2}(\nabla\widetilde{\boldsymbol{u}} + \nabla^{\mathsf{T}}\widetilde{\boldsymbol{u}}) \\ & \epsilon\,\mathrm{div}\,\widetilde{\boldsymbol{u}} = 0 \end{array}$$

Generic setting and key features

Generic visco-plastic behaviour: $\phi(\boldsymbol{d}) = \phi_{\text{visc}}(\boldsymbol{d}) + \phi_{\text{plast}}(\boldsymbol{d})$ where:

- **viscous part** ϕ_{visc} is strictly convex (homogeneous of degree $m+1>1$)
- **plastic part** ϕ_{plast} is homogeneous of degree 1. i.e. $\phi^*_{\text{plast}}(\boldsymbol{\sigma}) = \delta_G(\boldsymbol{\sigma})$ is the indicator of a convex set G containing 0

Behaviour at small velocities: introduce $\widetilde{\boldsymbol{u}} = \boldsymbol{u}/\epsilon$:

$$\begin{array}{ll} \displaystyle\min_{\widetilde{\boldsymbol{u}}} & \displaystyle\int_\Omega \left(\phi_{\text{visc}}(\epsilon\widetilde{\boldsymbol{d}}) + \phi_{\text{plast}}(\epsilon\widetilde{\boldsymbol{d}})\right) \,\mathrm{d}\Omega - \int_\Omega \boldsymbol{f}\cdot\epsilon\widetilde{\boldsymbol{u}}\,\mathrm{d}\Omega \\ \text{s.t.} & \epsilon\widetilde{\boldsymbol{d}} = \epsilon\frac{1}{2}(\nabla\widetilde{\boldsymbol{u}} + \nabla^{\mathsf{T}}\widetilde{\boldsymbol{u}}) \\ & \epsilon\,\operatorname{div}\widetilde{\boldsymbol{u}} = 0 \end{array}$$

$$\underset{\epsilon\to 0}{\longrightarrow}\quad \begin{array}{ll} \displaystyle\min_{\widetilde{\boldsymbol{u}}} & \displaystyle\int_\Omega \phi_{\text{plast}}(\widetilde{\boldsymbol{d}})\,\mathrm{d}\Omega - \int_\Omega \boldsymbol{f}\cdot\widetilde{\boldsymbol{u}}\,\mathrm{d}\Omega \\ \text{s.t.} & \widetilde{\boldsymbol{d}} = \frac{1}{2}(\nabla\widetilde{\boldsymbol{u}} + \nabla^{\mathsf{T}}\widetilde{\boldsymbol{u}}) \\ & \operatorname{div}\widetilde{\boldsymbol{u}} = 0 \end{array}$$

Generic setting and key features

Generic visco-plastic behaviour: $\phi(\boldsymbol{d}) = \phi_{\text{visc}}(\boldsymbol{d}) + \phi_{\text{plast}}(\boldsymbol{d})$ where:

- **viscous part** ϕ_{visc} is strictly convex (homogeneous of degree $m+1>1$)
- **plastic part** ϕ_{plast} is homogeneous of degree 1. i.e. $\phi^*_{\text{plast}}(\boldsymbol{\sigma}) = \delta_G(\boldsymbol{\sigma})$ is the indicator of a convex set G containing 0

Behaviour at small velocities: introduce $\widetilde{\boldsymbol{u}} = \boldsymbol{u}/\epsilon$:

$$\begin{array}{rll} & \displaystyle\min_{\widetilde{\boldsymbol{u}}} & \displaystyle\int_\Omega \left(\phi_{\text{visc}}(\epsilon\widetilde{\boldsymbol{d}}) + \phi_{\text{plast}}(\epsilon\widetilde{\boldsymbol{d}})\right) \,\mathrm{d}\Omega - \int_\Omega \boldsymbol{f}\cdot\epsilon\widetilde{\boldsymbol{u}}\,\mathrm{d}\Omega \\ & \text{s.t.} & \epsilon\widetilde{\boldsymbol{d}} = \epsilon\frac{1}{2}(\nabla\widetilde{\boldsymbol{u}} + \nabla^\mathsf{T}\widetilde{\boldsymbol{u}}) \\ & & \epsilon \operatorname{div}\widetilde{\boldsymbol{u}} = 0 \\ & \displaystyle\min_{\widetilde{\boldsymbol{u}}} & \displaystyle\int_\Omega \phi_{\text{plast}}(\widetilde{\boldsymbol{d}})\,\mathrm{d}\Omega - \int_\Omega \boldsymbol{f}\cdot\widetilde{\boldsymbol{u}}\,\mathrm{d}\Omega \\ \xrightarrow[\epsilon\to 0]{} & \text{s.t.} & \widetilde{\boldsymbol{d}} = \frac{1}{2}(\nabla\widetilde{\boldsymbol{u}} + \nabla^\mathsf{T}\widetilde{\boldsymbol{u}}) \\ & & \operatorname{div}\widetilde{\boldsymbol{u}} = 0 \end{array}$$

This is a **limit analysis problem** which has **no solution** if $\boldsymbol{f} \leq \boldsymbol{f}^+ \Rightarrow$ **no flow**

Generic setting and key features

Generic visco-plastic behaviour: $\phi(\boldsymbol{d}) = \phi_{\text{visc}}(\boldsymbol{d}) + \phi_{\text{plast}}(\boldsymbol{d})$ where:

- **viscous part** ϕ_{visc} is strictly convex (homogeneous of degree $m+1>1$)
- **plastic part** ϕ_{plast} is homogeneous of degree 1. i.e. $\phi^*_{\text{plast}}(\boldsymbol{\sigma}) = \delta_G(\boldsymbol{\sigma})$ is the indicator of a convex set G containing 0

Behaviour at small velocities: introduce $\widetilde{\boldsymbol{u}} = \boldsymbol{u}/\epsilon$:

$$\begin{array}{rl} \displaystyle\min_{\widetilde{\boldsymbol{u}}} & \displaystyle\int_\Omega \left(\phi_{\text{visc}}(\epsilon\widetilde{\boldsymbol{d}}) + \phi_{\text{plast}}(\epsilon\widetilde{\boldsymbol{d}})\right) \,d\Omega - \int_\Omega \boldsymbol{f}\cdot\epsilon\widetilde{\boldsymbol{u}}\,d\Omega \\ \text{s.t.} & \epsilon\widetilde{\boldsymbol{d}} = \epsilon\frac{1}{2}(\nabla\widetilde{\boldsymbol{u}} + \nabla^{\mathsf{T}}\widetilde{\boldsymbol{u}}) \\ & \epsilon\,\operatorname{div}\widetilde{\boldsymbol{u}} = 0 \end{array}$$

$$\underset{\epsilon\to 0}{\longrightarrow}\quad \begin{array}{rl} \displaystyle\min_{\widetilde{\boldsymbol{u}}} & \displaystyle\int_\Omega \phi_{\text{plast}}(\widetilde{\boldsymbol{d}})\,d\Omega - \int_\Omega \boldsymbol{f}\cdot\widetilde{\boldsymbol{u}}\,d\Omega \\ \text{s.t.} & \widetilde{\boldsymbol{d}} = \frac{1}{2}(\nabla\widetilde{\boldsymbol{u}} + \nabla^{\mathsf{T}}\widetilde{\boldsymbol{u}}) \\ & \operatorname{div}\widetilde{\boldsymbol{u}} = 0 \end{array}$$

This is a **limit analysis problem** which has **no solution** if $\boldsymbol{f} \leq \boldsymbol{f}^+ \Rightarrow$ **no flow**

Similarly, without any forcing: **return to rest** in **finite time**

Dual variational principle

Dual variational problem: using standard **convex duality**:

$$\begin{aligned} -(P) = \min_{\boldsymbol{s}} \quad & \int_\Omega \phi^*(\boldsymbol{s})\, \mathrm{d}\Omega \\ \text{s.t.} \quad & \operatorname{div} \boldsymbol{s} - \nabla p + \boldsymbol{f} = 0 \end{aligned}$$

where

$$\phi^*(\boldsymbol{s}) = (\phi_{\text{visc}} + \phi_{\text{plast}})^*(\boldsymbol{s}) = \phi^*_{\text{visc}} \square \phi^*_{\text{plast}}(\boldsymbol{s}) = \inf_{\boldsymbol{\tau} \in G} \phi^*_{\text{visc}}(\boldsymbol{s} - \boldsymbol{\tau})$$

Dual variational principle

Dual variational problem: using standard **convex duality**:

$$\begin{aligned} -(P) = \min_{\boldsymbol{s}} \quad & \int_\Omega \phi^*_{\text{visc}}(\boldsymbol{s}-\boldsymbol{\tau})\,\mathrm{d}\Omega \\ \text{s.t.} \quad & \operatorname{div}\boldsymbol{s} - \nabla p + \boldsymbol{f} = 0 \\ & \|\boldsymbol{\tau}\| \leq \sqrt{2}\tau_0 \end{aligned}$$

where

$$\phi^*(\boldsymbol{s}) = (\phi_{\text{visc}} + \phi_{\text{plast}})^*(\boldsymbol{s}) = \phi^*_{\text{visc}}\Box\phi^*_{\text{plast}}(\boldsymbol{s}) = \inf_{\boldsymbol{\tau}\in G} \phi^*_{\text{visc}}(\boldsymbol{s}-\boldsymbol{\tau})$$

Dual variational principle

Dual variational problem: using standard **convex duality**:

$$\begin{array}{rl} -(P) = \min\limits_{\boldsymbol{s}} & \displaystyle\int_\Omega \phi^*_{\text{visc}}(\boldsymbol{s}-\boldsymbol{\tau})\,\mathrm{d}\Omega \\ \text{s.t.} & \operatorname{div}\boldsymbol{s} - \nabla p + \boldsymbol{f} = 0 \\ & \|\boldsymbol{\tau}\| \leq \sqrt{2}\tau_0 \end{array}$$

where

$$\phi^*(\boldsymbol{s}) = (\phi_{\text{visc}} + \phi_{\text{plast}})^*(\boldsymbol{s}) = \phi^*_{\text{visc}}\square\phi^*_{\text{plast}}(\boldsymbol{s}) = \inf_{\boldsymbol{\tau}\in G} \phi^*_{\text{visc}}(\boldsymbol{s}-\boldsymbol{\tau})$$

Bingham:

$$\phi^*_{\text{visc}}(\boldsymbol{s}-\boldsymbol{\tau}) = \frac{1}{4\eta}\|\boldsymbol{s}-\boldsymbol{\tau}\|^2$$

Herschel-Bulkley:

$$\phi^*_{\text{visc}}(\boldsymbol{s}-\boldsymbol{\tau}) = \frac{m}{(m+1)K^{1/m}2^{(m+1)/2m}}\|\boldsymbol{s}-\boldsymbol{\tau}\|^{1+1/m}$$

Newtonian:

$$\boldsymbol{\tau} = 0$$

Dual variational principle

Dual variational problem: using standard **convex duality**:

$$
\begin{aligned}
-(P) = \min_{\boldsymbol{s}} \quad & \int_\Omega \phi^*_{\text{visc}}(\boldsymbol{s} - \boldsymbol{\tau})\,\mathrm{d}\Omega \\
\text{s.t.} \quad & \operatorname{div} \boldsymbol{s} - \nabla p + \boldsymbol{f} = 0 \\
& \|\boldsymbol{\tau}\| \leq \sqrt{2}\tau_0
\end{aligned}
$$

where

$$
\phi^*(\boldsymbol{s}) = (\phi_{\text{visc}} + \phi_{\text{plast}})^*(\boldsymbol{s}) = \phi^*_{\text{visc}} \square \phi^*_{\text{plast}}(\boldsymbol{s}) = \inf_{\boldsymbol{\tau}\in G} \phi^*_{\text{visc}}(\boldsymbol{s} - \boldsymbol{\tau})
$$

Bingham:

$$
\phi^*_{\text{visc}}(\boldsymbol{s} - \boldsymbol{\tau}) = \frac{1}{4\eta}\|\boldsymbol{s} - \boldsymbol{\tau}\|^2
$$

Herschel-Bulkley:

$$
\phi^*_{\text{visc}}(\boldsymbol{s} - \boldsymbol{\tau}) = \frac{m}{(m+1)K^{1/m}2^{(m+1)/2m}}\|\boldsymbol{s} - \boldsymbol{\tau}\|^{1+1/m}
$$

Newtonian:

$$
\boldsymbol{\tau} = 0
$$

Mathematical structure very similar to **contact/friction**, **elastoplasticity**

Poiseuille flow

Analytical solution for plane Poiseuille flow:
$\sigma_{xz} = f(z - H/2)$

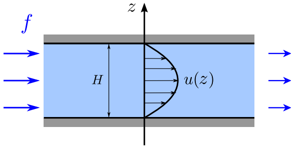

The Bingham number

$$\mathrm{Bi} = \frac{\tau_0 U}{\eta H}$$

Newtonian $= 0 \leq \mathrm{Bi} \leq \infty =$ **perfectly plastic**

Poiseuille flow

Analytical solution for plane Poiseuille flow:
$\sigma_{xz} = f(z - H/2)$

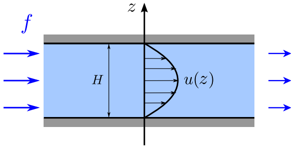

The Bingham number

$$\mathrm{Bi} = \frac{\tau_0 U}{\eta H}$$

Newtonian $= 0 \leq \mathrm{Bi} \leq \infty =$ **perfectly plastic**

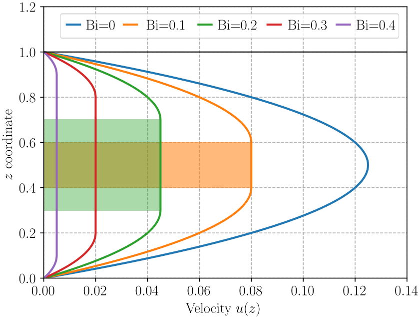

shear near the edges: parabolic Newtonian profile
near the center: rigid plug region with uniform velocity
solid region : $0.5 - \mathrm{Bi} \leq z/H \leq \mathrm{Bi} + 0.5$
$\Rightarrow$ **flow stops** when $\mathrm{Bi} = \mathrm{Bi}_c = 0.5$

Bi-dimensional flows in Hele-Shaw cells [Bleyer, 2022]

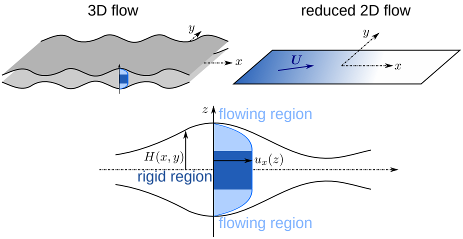

Bi-dimensional flows in Hele-Shaw cells [Bleyer, 2022]

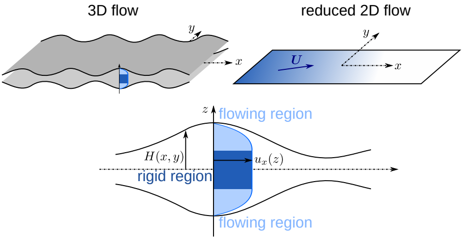

3D-2D **dimensionality reduction** hypotheses:

- the transverse velocity is negligible: $u_z \approx 0$
- transverse directions are much larger than in-plane variations $\|\boldsymbol{u}_{,x}\|, \|\boldsymbol{u}_{,y}\| \ll \|\boldsymbol{u}_{,z}\|$
- no-slip condition along walls
- inertia and body forces can be ignored

Bi-dimensional flows in Hele-Shaw cells [Bleyer, 2022]

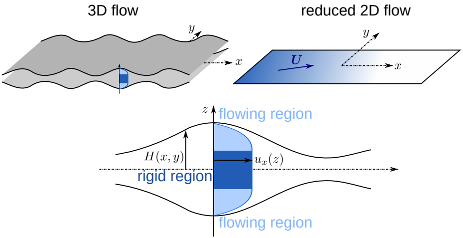

3D-2D **dimensionality reduction** hypotheses:

- the transverse velocity is negligible: $u_z \approx 0$
- transverse directions are much larger than in-plane variations $\|\boldsymbol{u}_{,x}\|, \|\boldsymbol{u}_{,y}\| \ll \|\boldsymbol{u}_{,z}\|$
- no-slip condition along walls
- inertia and body forces can be ignored

results in a linearly varying shear stress field

$$\boldsymbol{\sigma}(x,y,z) \approx \begin{bmatrix} 0 & 0 & \tau_x \\ 0 & 0 & \tau_y \\ \tau_x & \tau_y & 0 \end{bmatrix}$$

$$\text{with } \boldsymbol{\tau}(x,y) = z\nabla p(x,y)$$

where $\boldsymbol{\tau}(x,y,z)$ is the anti-plane shear stress vector and $p(x,y)$ is the fluid pressure

Determining effective potentials

Hele-Shaw effective behaviour can be described through **effective potentials**:

- either in **stress-based** form $\Psi(\boldsymbol{G})$ with the pressure gradient $\boldsymbol{G}(x, y) = -\nabla p(x, y)$

Determining effective potentials

Hele-Shaw effective behaviour can be described through **effective potentials**:

- either in **stress-based** form $\Psi(\boldsymbol{G})$ with the pressure gradient $\boldsymbol{G}(x,y) = -\nabla p(x,y)$
- or, in **velocity-based** form $\Phi(\boldsymbol{U})$ of the macroscopic velocity $\boldsymbol{U}(x,y)$

with Legendre-Fenchel duality $\Psi = \Phi^*$ with:

$$\boldsymbol{U} \in \partial_{\boldsymbol{G}}\Psi(\boldsymbol{G}) \quad , \quad \boldsymbol{G} \in \partial_{\boldsymbol{U}}\Phi(\boldsymbol{U})$$

Determining effective potentials

Hele-Shaw effective behaviour can be described through **effective potentials**:

- either in **stress-based** form $\Psi(\boldsymbol{G})$ with the pressure gradient $\boldsymbol{G}(x,y) = -\nabla p(x,y)$
- or, in **velocity-based** form $\Phi(\boldsymbol{U})$ of the macroscopic velocity $\boldsymbol{U}(x,y)$

with Legendre-Fenchel duality $\Psi = \Phi^*$ with:

$$\boldsymbol{U} \in \partial_{\boldsymbol{G}}\Psi(\boldsymbol{G}) \quad , \quad \boldsymbol{G} \in \partial_{\boldsymbol{U}}\Phi(\boldsymbol{U})$$

Stress potential:

$$\Psi(\boldsymbol{G}) = \frac{1}{2H}\int_{-H}^{H} \psi(\boldsymbol{\sigma}(x,y,z))\,\mathrm{d}z$$

where ψ is the 3D stress-based potential of the constituting fluid.

Determining effective potentials

Hele-Shaw effective behaviour can be described through **effective potentials**:

- either in **stress-based** form $\Psi(\boldsymbol{G})$ with the pressure gradient $\boldsymbol{G}(x, y) = -\nabla p(x, y)$
- or, in **velocity-based** form $\Phi(\boldsymbol{U})$ of the macroscopic velocity $\boldsymbol{U}(x, y)$

with Legendre-Fenchel duality $\Psi = \Phi^*$ with:

$$\boldsymbol{U} \in \partial_{\boldsymbol{G}}\Psi(\boldsymbol{G}) \quad , \quad \boldsymbol{G} \in \partial_{\boldsymbol{U}}\Phi(\boldsymbol{U})$$

Stress potential:

$$\Psi(\boldsymbol{G}) = \frac{1}{2H}\int_{-H}^{H} \psi(\boldsymbol{\sigma}(x, y, z))\,\mathrm{d}z$$

where ψ is the 3D stress-based potential of the constituting fluid.

Newtonian fluid

$$\phi(\boldsymbol{d}) = \eta \boldsymbol{d} : \boldsymbol{d},\ \psi(\boldsymbol{\sigma}) = \phi^*(\boldsymbol{d}) = \frac{\boldsymbol{\sigma} : \boldsymbol{\sigma}}{4\eta} \Rightarrow \Psi(\boldsymbol{G}) = \int_{-H}^{H} \frac{1}{4\eta H} z^2 \boldsymbol{G} \cdot \boldsymbol{G}\,\mathrm{d}z = \frac{H^2}{6\eta}\boldsymbol{G} \cdot \boldsymbol{G}$$

we recover the **Darcy equation** between two parallel plates:

$$\boldsymbol{U} = \partial_{\boldsymbol{G}}\Psi(\boldsymbol{G}) = \frac{H^2}{3\eta}\boldsymbol{G}$$

The velocity effective potential

obtained via Legendre-Fenchel transform:

$$\begin{aligned}\Phi(\boldsymbol{U}) &= \sup_{\boldsymbol{G}}\{\boldsymbol{U}\cdot\boldsymbol{G} - \Psi(\boldsymbol{G})\}\\ &= \inf_{\boldsymbol{\gamma}(z)} \quad \frac{1}{2H}\int_{-H}^{H}\phi(\boldsymbol{d}(z))\,\mathrm{d}z\\ &\text{s.t.} \quad \boldsymbol{d}(z) = \begin{bmatrix} 0 & 0 & \gamma_x(z)\\ 0 & 0 & \gamma_y(z)\\ \gamma_x(z) & \gamma_y(z) & 0\end{bmatrix}\\ &\qquad\quad \boldsymbol{U} + \frac{1}{2H}\int_{-H}^{H} z\boldsymbol{\gamma}(z)\,\mathrm{d}z = 0\end{aligned}$$

The velocity effective potential

obtained via Legendre-Fenchel transform:

$$\begin{aligned}
\Phi(\boldsymbol{U}) &= \sup_{\boldsymbol{G}}\{\boldsymbol{U}\cdot\boldsymbol{G} - \Psi(\boldsymbol{G})\} \\
&= \inf_{\boldsymbol{\gamma}(z)} \quad \frac{1}{2H}\int_{-H}^{H}\phi(\boldsymbol{d}(z))\,\mathrm{d}z \\
&\quad \text{s.t.} \quad \boldsymbol{d}(z) = \begin{bmatrix} 0 & 0 & \gamma_x(z) \\ 0 & 0 & \gamma_y(z) \\ \gamma_x(z) & \gamma_y(z) & 0 \end{bmatrix} \\
&\qquad\qquad \boldsymbol{U} + \frac{1}{2H}\int_{-H}^{H} z\boldsymbol{\gamma}(z)\,\mathrm{d}z = 0
\end{aligned}$$

Interpreting $\boldsymbol{\gamma}(z) = \boldsymbol{u}_{,z}$ as the local strain rate, the last constraint is equivalent to:

$$\boldsymbol{U} + \frac{1}{2H}\int_{-H}^{H} z\boldsymbol{u}_{,z}\,\mathrm{d}z = \boldsymbol{U} - \frac{1}{2H}\int_{-H}^{H}\boldsymbol{u}\,\mathrm{d}z = 0$$

The velocity effective potential

obtained via Legendre-Fenchel transform:

$$\begin{aligned}\Phi(\boldsymbol{U}) &= \sup_{\boldsymbol{G}}\{\boldsymbol{U}\cdot\boldsymbol{G} - \Psi(\boldsymbol{G})\}\\ &= \inf_{\boldsymbol{\gamma}(z)} \quad \frac{1}{2H}\int_{-H}^{H}\phi(\boldsymbol{d}(z))\,\mathrm{d}z\\ &\quad \text{s.t.} \quad \boldsymbol{d}(z) = \begin{bmatrix} 0 & 0 & \gamma_x(z)\\ 0 & 0 & \gamma_y(z)\\ \gamma_x(z) & \gamma_y(z) & 0\end{bmatrix}\\ &\qquad\qquad \boldsymbol{U} + \frac{1}{2H}\int_{-H}^{H} z\boldsymbol{\gamma}(z)\,\mathrm{d}z = 0\end{aligned}$$

Interpreting $\boldsymbol{\gamma}(z) = \boldsymbol{u}_{,z}$ as the local strain rate, the last constraint is equivalent to:

$$\boldsymbol{U} + \frac{1}{2H}\int_{-H}^{H} z\boldsymbol{u}_{,z}\,\mathrm{d}z = \boldsymbol{U} - \frac{1}{2H}\int_{-H}^{H}\boldsymbol{u}\,\mathrm{d}z = 0$$

Bingham case:

$$\begin{aligned}\Phi(\boldsymbol{U}) = \inf_{\boldsymbol{\gamma}(z)} &\quad \frac{1}{2H}\int_{-H}^{H}\left(\frac{\eta}{2}\|\boldsymbol{\gamma}(z)\|^2 + \tau_0\|\boldsymbol{\gamma}(z)\|\right)\,\mathrm{d}z\\ \text{s.t.} &\quad \boldsymbol{U} + \frac{1}{2H}\int_{-H}^{H} z\boldsymbol{\gamma}(z)\,\mathrm{d}z = 0\end{aligned}$$

A tractable approximation

No closed-form expression

Approximation: $\boldsymbol{\gamma}_i = \boldsymbol{\gamma}(z_i)$ at $i = 1, \dots, m$ quadrature points z_i:

$$\begin{aligned}\Phi_m(\boldsymbol{U}) = \inf_{\boldsymbol{\gamma}_i} \quad & \sum_{i=1}^m \omega_i \left(\frac{\eta}{2}\|\boldsymbol{\gamma}_i\|^2 + \tau_0\|\boldsymbol{\gamma}_i\|\right) \\ \text{s.t.} \quad & \boldsymbol{U} + H\sum_{i=1}^m \omega_i \xi_i \boldsymbol{\gamma}_i = 0\end{aligned}$$

A tractable approximation

No closed-form expression

Approximation: $\gamma_i = \gamma(z_i)$ at $i = 1, \dots, m$ quadrature points z_i:

$$\Phi_m(\boldsymbol{U}) = \inf_{\boldsymbol{\gamma}_i} \quad \sum_{i=1}^{m} \omega_i \left(\frac{\eta}{2} \|\boldsymbol{\gamma}_i\|^2 + \tau_0 \|\boldsymbol{\gamma}_i\| \right)$$

$$\text{s.t.} \quad \boldsymbol{U} + H \sum_{i=1}^{m} \omega_i \xi_i \boldsymbol{\gamma}_i = 0$$

Flow curves: norm of the pressure gradient $G = \|\boldsymbol{G}\|$ as a function of filtration velocity magnitude $U = \|\boldsymbol{U}\|$

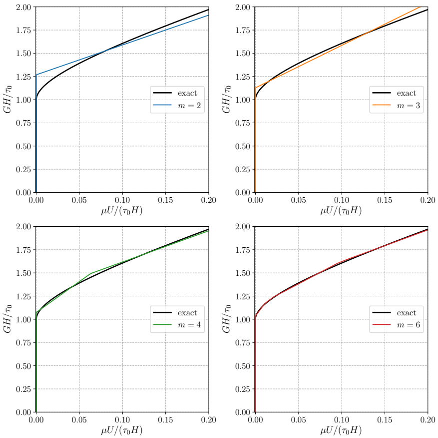

Flow in a random medium

Hele-Shaw cell with **spatially varying height**

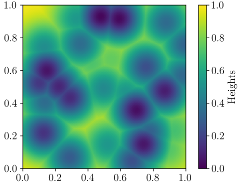

$$
\begin{aligned}
\min_{\boldsymbol{U}} \quad & \int_\Omega \Phi_m(\boldsymbol{U}) \mathrm{d}\Omega - \int_{\partial\Omega_\mathrm{D}} p_0 \boldsymbol{U} \cdot \boldsymbol{n} \, \mathrm{d}S \\
\text{s.t.} \quad & \operatorname{div} \boldsymbol{U} = 0 \text{ in } \Omega \\
& \boldsymbol{U} \cdot \boldsymbol{n} = q \text{ on } \partial\Omega_\mathrm{N}
\end{aligned}
$$

Flow in a random medium

Hele-Shaw cell with **spatially varying height**

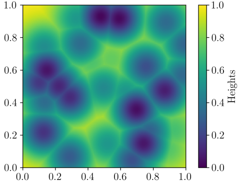

$$
\begin{aligned}
\min_{\boldsymbol{U}} \quad & \int_\Omega \Phi_m(\boldsymbol{U})\,\mathrm{d}\Omega - \int_{\partial\Omega_\mathrm{D}} p_0 \boldsymbol{U}\cdot\boldsymbol{n}\,\mathrm{d}S \\
\text{s.t.} \quad & \operatorname{div}\boldsymbol{U} = 0 \text{ in } \Omega \\
& \boldsymbol{U}\cdot\boldsymbol{n} = q \text{ on } \partial\Omega_\mathrm{N}
\end{aligned}
$$

Horizontal filtration velocity maps for different imposed pressure gradients $\overline{G}$

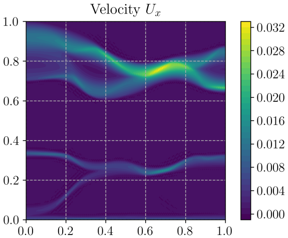

$\overline{G} = 2$

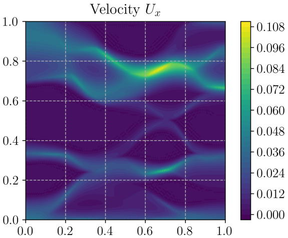

$\overline{G} = 2.5$

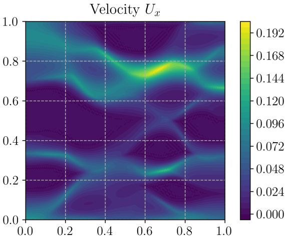

$\overline{G} = 3$

Outline

Numerical difficulties and mitigation strategies

The **existence of yield stress** poses numerical challenges:

- **non-smooth** potential $\Rightarrow$ Newton methods generally fail
- **unknown rigid regions**
- **unknown stress** in rigid regions

Numerical difficulties and mitigation strategies

The **existence of yield stress** poses numerical challenges:

- **non-smooth** potential $\Rightarrow$ Newton methods generally fail
- **unknown rigid regions**
- **unknown stress** in rigid regions

Bi-viscous regularization: abandon the idea of a **yield stress**, replace rigid regions with **high viscosity** regions e.g. [Bercovier and Engelman, 1980]

$$\boldsymbol{\sigma} = 2\eta \boldsymbol{d} + \sqrt{2}\tau_0 \frac{\boldsymbol{d}}{\|\boldsymbol{d}\|} \quad \Rightarrow \quad \boldsymbol{\sigma}_\epsilon = 2\eta \boldsymbol{d} + \sqrt{2}\tau_0 \frac{\boldsymbol{d}}{\sqrt{\|\boldsymbol{d}\|^2 + \epsilon^2}} = 2\eta_\epsilon(\|\boldsymbol{d}\|)\boldsymbol{d}$$

Numerical difficulties and mitigation strategies

The **existence of yield stress** poses numerical challenges:

- **non-smooth** potential $\Rightarrow$ Newton methods generally fail
- **unknown rigid regions**
- **unknown stress** in rigid regions

Bi-viscous regularization: abandon the idea of a **yield stress**, replace rigid regions with **high viscosity** regions e.g. [Bercovier and Engelman, 1980]

$$\boldsymbol{\sigma} = 2\eta \boldsymbol{d} + \sqrt{2}\tau_0 \frac{\boldsymbol{d}}{\|\boldsymbol{d}\|} \quad \Rightarrow \quad \boldsymbol{\sigma}_\epsilon = 2\eta \boldsymbol{d} + \sqrt{2}\tau_0 \frac{\boldsymbol{d}}{\sqrt{\|\boldsymbol{d}\|^2 + \epsilon^2}} = 2\eta_\epsilon(\|\boldsymbol{d}\|)\boldsymbol{d}$$

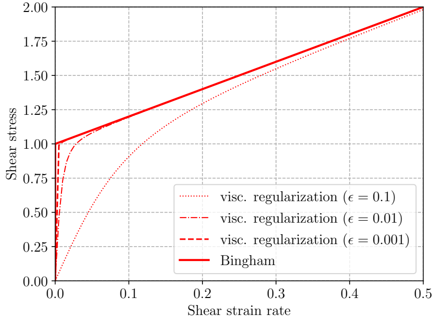

Numerical difficulties and mitigation strategies

The **existence of yield stress** poses numerical challenges:

- **non-smooth** potential $\Rightarrow$ Newton methods generally fail
- **unknown rigid regions**
- **unknown stress** in rigid regions

Bi-viscous regularization: abandon the idea of a **yield stress**, replace rigid regions with **high viscosity** regions e.g. [Bercovier and Engelman, 1980]

$$\boldsymbol{\sigma} = 2\eta\boldsymbol{d} + \sqrt{2}\tau_0\frac{\boldsymbol{d}}{\|\boldsymbol{d}\|} \quad \Rightarrow \quad \boldsymbol{\sigma}_\epsilon = 2\eta\boldsymbol{d} + \sqrt{2}\tau_0\frac{\boldsymbol{d}}{\sqrt{\|\boldsymbol{d}\|^2+\epsilon^2}} = 2\eta_\epsilon(\|\boldsymbol{d}\|)\boldsymbol{d}$$

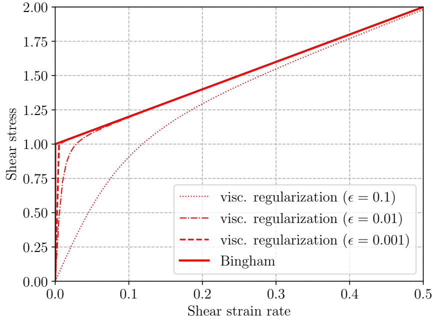

Problems:

- **poor conditioning** when $\epsilon \to 0$
- no **real rigid region**, large sensitivity to the chosen threshold
- **no convergence** of the stress $\boldsymbol{\sigma}_\epsilon \not\to \boldsymbol{\sigma}$
- return to rest in **finite time** is **lost**

Augmented Lagrangian approaches

Going back to the Lagrangian saddle point-problem $\max_{\boldsymbol{s},p} \min_{\boldsymbol{u},\boldsymbol{d}} \mathcal{L}(\boldsymbol{u}, \boldsymbol{d}, \boldsymbol{s}, p)$ where:

$$\mathcal{L}(\boldsymbol{u}, \boldsymbol{d}, \boldsymbol{s}, p) = \int_\Omega (\phi(\boldsymbol{d}) - p \operatorname{div} \boldsymbol{u} - \boldsymbol{s} : (\boldsymbol{d} - \nabla^s \boldsymbol{u}))\, \mathrm{d}\Omega - \mathcal{P}_{\text{ext}}(\boldsymbol{u})$$

Augmented Lagrangian approaches

Going back to the Lagrangian saddle point-problem $\max_{\boldsymbol{s},p} \min_{\boldsymbol{u},\boldsymbol{d}} \mathcal{L}(\boldsymbol{u}, \boldsymbol{d}, \boldsymbol{s}, p)$ where:

$$\mathcal{L}(\boldsymbol{u}, \boldsymbol{d}, \boldsymbol{s}, p) = \int_\Omega (\phi(\boldsymbol{d}) - p \operatorname{div} \boldsymbol{u} - \boldsymbol{s} : (\boldsymbol{d} - \nabla^s \boldsymbol{u})) \, \mathrm{d}\Omega - \mathcal{P}_{\text{ext}}(\boldsymbol{u})$$

Introduce an **augmented** Lagrangian for $r > 0$:

$$\mathcal{L}_r(\boldsymbol{u}, \boldsymbol{d}, \boldsymbol{s}, p) = \int_\Omega \left(\phi(\boldsymbol{d}) - p \operatorname{div} \boldsymbol{u} - \boldsymbol{s} : (\boldsymbol{d} - \nabla^s \boldsymbol{u}) + \frac{r}{2}(\boldsymbol{d} - \nabla^s \boldsymbol{u})^2\right) \mathrm{d}\Omega - \mathcal{P}_{\text{ext}}(\boldsymbol{u})$$

Augmented Lagrangian approaches

Going back to the Lagrangian saddle point-problem $\max_{\boldsymbol{s},p} \min_{\boldsymbol{u},\boldsymbol{d}} \mathcal{L}(\boldsymbol{u}, \boldsymbol{d}, \boldsymbol{s}, p)$ where:

$$\mathcal{L}(\boldsymbol{u}, \boldsymbol{d}, \boldsymbol{s}, p) = \int_\Omega (\phi(\boldsymbol{d}) - p \operatorname{div} \boldsymbol{u} - \boldsymbol{s} : (\boldsymbol{d} - \nabla^s \boldsymbol{u})) \,\mathrm{d}\Omega - \mathcal{P}_{\text{ext}}(\boldsymbol{u})$$

Introduce an **augmented** Lagrangian for $r > 0$:

$$\mathcal{L}_r(\boldsymbol{u}, \boldsymbol{d}, \boldsymbol{s}, p) = \int_\Omega \left(\phi(\boldsymbol{d}) - p \operatorname{div} \boldsymbol{u} - \boldsymbol{s} : (\boldsymbol{d} - \nabla^s \boldsymbol{u}) + \frac{r}{2}(\boldsymbol{d} - \nabla^s \boldsymbol{u})^2\right) \,\mathrm{d}\Omega - \mathcal{P}_{\text{ext}}(\boldsymbol{u})$$

solved using **Uzawa's method**:

$$\boldsymbol{u}_{n+1}, p_{n+1} = \min_{\boldsymbol{u},\boldsymbol{p}} \mathcal{L}_r(\boldsymbol{u}, \boldsymbol{d}_n, \boldsymbol{s}_n, p) \tag{5}$$

$$\boldsymbol{d}_{n+1} = \min_{\boldsymbol{d}} \mathcal{L}_r(\boldsymbol{u}_{n+1}, \boldsymbol{d}, \boldsymbol{s}_n, p_{n+1}) \tag{6}$$

$$\boldsymbol{s}_{n+1} = \boldsymbol{s}_n + r(\nabla^s \boldsymbol{u}_{n+1} - \boldsymbol{d}_{n+1}) \tag{7}$$

Augmented Lagrangian approaches

Going back to the Lagrangian saddle point-problem $\max_{\boldsymbol{s},p} \min_{\boldsymbol{u},\boldsymbol{d}} \mathcal{L}(\boldsymbol{u}, \boldsymbol{d}, \boldsymbol{s}, p)$ where:

$$\mathcal{L}(\boldsymbol{u}, \boldsymbol{d}, \boldsymbol{s}, p) = \int_\Omega (\phi(\boldsymbol{d}) - p \operatorname{div} \boldsymbol{u} - \boldsymbol{s} : (\boldsymbol{d} - \nabla^s \boldsymbol{u})) \,\mathrm{d}\Omega - \mathcal{P}_{\text{ext}}(\boldsymbol{u})$$

Introduce an **augmented** Lagrangian for $r > 0$:

$$\mathcal{L}_r(\boldsymbol{u}, \boldsymbol{d}, \boldsymbol{s}, p) = \int_\Omega \left(\phi(\boldsymbol{d}) - p \operatorname{div} \boldsymbol{u} - \boldsymbol{s} : (\boldsymbol{d} - \nabla^s \boldsymbol{u}) + \frac{r}{2}(\boldsymbol{d} - \nabla^s \boldsymbol{u})^2\right) \,\mathrm{d}\Omega - \mathcal{P}_{\text{ext}}(\boldsymbol{u})$$

solved using **Uzawa's method**:

$$\boldsymbol{u}_{n+1}, p_{n+1} = \min_{\boldsymbol{u},\boldsymbol{p}} \mathcal{L}_r(\boldsymbol{u}, \boldsymbol{d}_n, \boldsymbol{s}_n, p) \tag{5}$$

$$\boldsymbol{d}_{n+1} = \min_{\boldsymbol{d}} \mathcal{L}_r(\boldsymbol{u}_{n+1}, \boldsymbol{d}, \boldsymbol{s}_n, p_{n+1}) \tag{6}$$

$$\boldsymbol{s}_{n+1} = \boldsymbol{s}_n + r(\nabla^s \boldsymbol{u}_{n+1} - \boldsymbol{d}_{n+1}) \tag{7}$$

(**??**) = **Stokes** problem of fixed viscosity r
(**??**) = **local** problem with closed form solution

$$\boldsymbol{d}_{n+1} = \frac{\boldsymbol{s}_n + r\nabla^s \boldsymbol{u}_{n+1}}{2\eta + r} \left\langle 1 - \frac{\sqrt{2}\tau_0}{\|\boldsymbol{s} + r\nabla^s \boldsymbol{u}\|} \right\rangle_+$$

Augmented Lagrangian approaches

Pros: easy to implement
Cons: **first-order** algorithm, residual convergence in $O(1/k)$

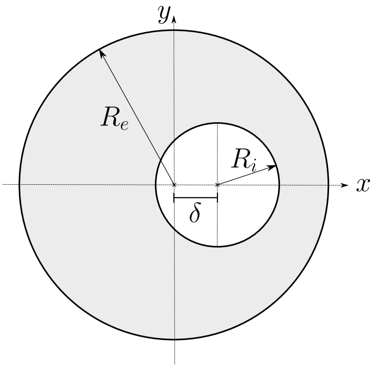

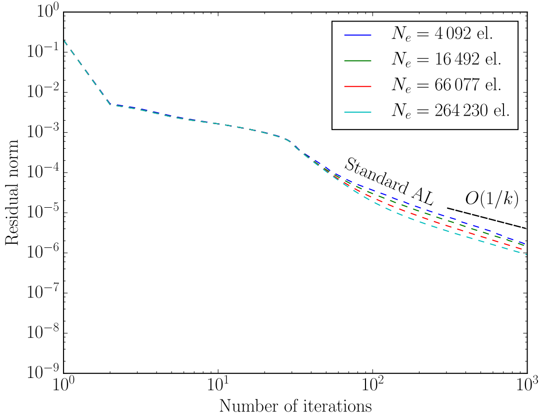

Augmented Lagrangian approaches

Pros: easy to implement
Cons: **first-order** algorithm, residual convergence in $O(1/k)$

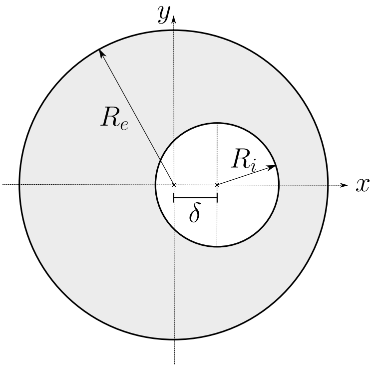

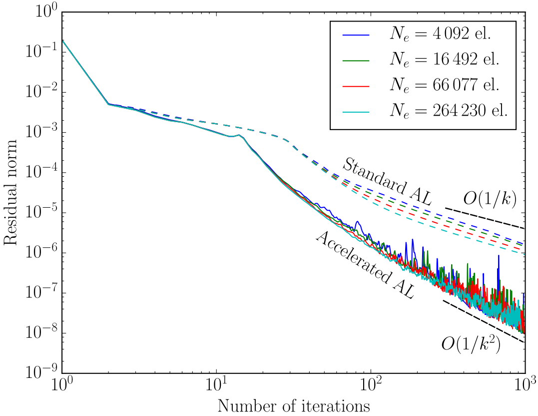

Accelerated versions reach $O(1/k^2)$ at most [Treskatis, 2016; Bleyer, 2017]

Augmented Lagrangian approaches

Pros: easy to implement
Cons: **first-order** algorithm, residual convergence in $O(1/k)$

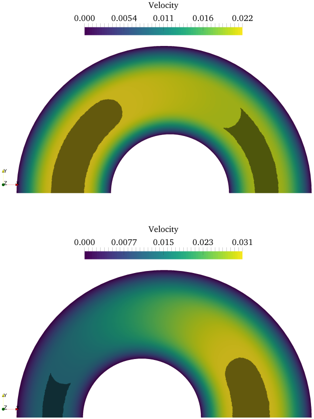

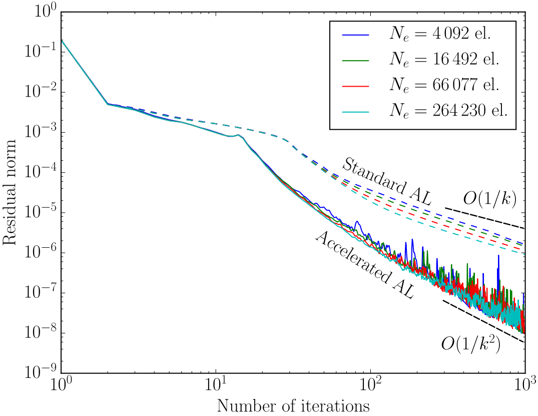

Accelerated versions reach $O(1/k^2)$ at most [Treskatis, 2016; Bleyer, 2017]

Mesh adaptation

Mesh adaptation based on **flowing status** [Kascavita et al., 2021]

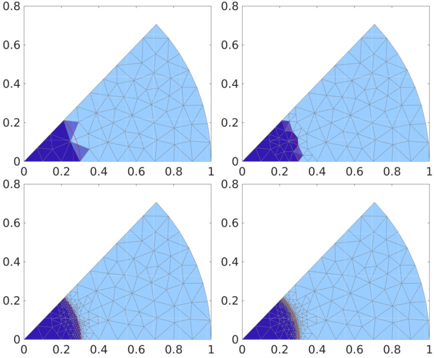

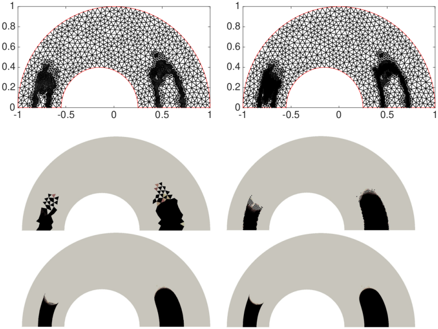

Dark blue = rigid region

Mesh adaptation

Mesh adaptation based on **anisotropic metric** [Roquet and Saramito, 2001]

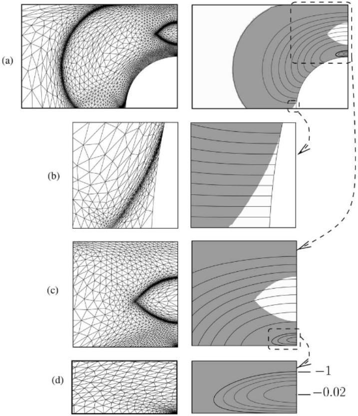

Flow past a cylinder [Roquet and Sarmito, 2003]

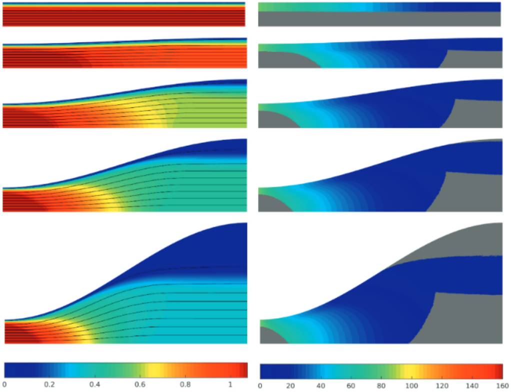

Flow past a wavy channel [Treskatis, 2018]

Outline

Linear and conic programming

Linear Programming :

$$
\begin{aligned}
\max \quad & \boldsymbol{c}^T\boldsymbol{x} \\
\text{s.t.} \quad & \boldsymbol{A}\boldsymbol{x} = \boldsymbol{b} \\
& \boldsymbol{x} \geq 0
\end{aligned}
$$

Linear and conic programming

Linear Programming :

$$
\begin{aligned}
\max \quad & \boldsymbol{c}^T\boldsymbol{x} \\
\text{s.t.} \quad & \boldsymbol{A}\boldsymbol{x} = \boldsymbol{b} \\
& \boldsymbol{x} \geq 0
\end{aligned}
$$

Linear programming solvers

- simplex algorithm [Dantzig et al., 1955] => exponential complexity
- interior point algorithm [Karmakar, 1984] => polynomial complexity

Linear and conic programming

Linear Programming :

$$\begin{aligned} \max \quad & \boldsymbol{c}^T \boldsymbol{x} \\ \text{s.t.} \quad & \boldsymbol{A}\boldsymbol{x} = \boldsymbol{b} \\ & \boldsymbol{x} \geq 0 \end{aligned}$$

Conic Programming :

$$\begin{aligned} \max \quad & \boldsymbol{c}^T \boldsymbol{x} \\ \text{s.t.} \quad & \boldsymbol{A}\boldsymbol{x} = \boldsymbol{b} \\ & \boldsymbol{x} \in \mathcal{K}^1 \times \ldots \times \mathcal{K}^p \end{aligned}$$

where $\mathcal{K}^j$ are **cones** e.g. :

Linear and conic programming

Linear Programming :

$$\begin{aligned} \max \quad & \boldsymbol{c}^T\boldsymbol{x} \\ \text{s.t.} \quad & \boldsymbol{A}\boldsymbol{x} = \boldsymbol{b} \\ & \boldsymbol{x} \geq 0 \end{aligned}$$

Conic Programming :

$$\begin{aligned} \max \quad & \boldsymbol{c}^T\boldsymbol{x} \\ \text{s.t.} \quad & \boldsymbol{A}\boldsymbol{x} = \boldsymbol{b} \\ & \boldsymbol{x} \in \mathcal{K}^1 \times \ldots \times \mathcal{K}^p \end{aligned}$$

where $\mathcal{K}^j$ are **cones** e.g. :

- positive orthant : $\mathcal{K}^j = \mathbb{R}^{n+} = \{\boldsymbol{x} \text{ s.t. } x_i \geq 0\} \Rightarrow$ LP

Linear and conic programming

Linear Programming :

$$\begin{aligned} \max \quad & \boldsymbol{c}^T\boldsymbol{x} \\ \text{s.t.} \quad & \boldsymbol{A}\boldsymbol{x} = \boldsymbol{b} \\ & \boldsymbol{x} \geq 0 \end{aligned}$$

Conic Programming :

$$\begin{aligned} \max \quad & \boldsymbol{c}^T\boldsymbol{x} \\ \text{s.t.} \quad & \boldsymbol{A}\boldsymbol{x} = \boldsymbol{b} \\ & \boldsymbol{x} \in \mathcal{K}^1 \times \ldots \times \mathcal{K}^p \end{aligned}$$

where $\mathcal{K}^j$ are **cones** e.g. :

- positive orthant : $\mathcal{K}^j = \mathbb{R}^{n+} = \{\boldsymbol{x} \text{ s.t. } x_i \geq 0\} \Rightarrow$ LP
- Lorentz second-order ("ice-cream") cone :

$$\mathcal{K}^j = \{\boldsymbol{x} = (x_0, \bar{\boldsymbol{x}}) \in \mathbb{R} \times \mathbb{R}^{n-1} \text{ s.t. } \|\bar{\boldsymbol{x}}\| \leq x_0\} \text{ => SOCP}$$

Linear and conic programming

Linear Programming :

$$\begin{array}{rl} \max & \boldsymbol{c}^T\boldsymbol{x} \\ \text{s.t.} & \boldsymbol{A}\boldsymbol{x} = \boldsymbol{b} \\ & \boldsymbol{x} \geq 0 \end{array}$$

Conic Programming :

$$\begin{array}{rl} \max & \boldsymbol{c}^T\boldsymbol{x} \\ \text{s.t.} & \boldsymbol{A}\boldsymbol{x} = \boldsymbol{b} \\ & \boldsymbol{x} \in \mathcal{K}^1 \times \ldots \times \mathcal{K}^p \end{array}$$

where $\mathcal{K}^j$ are **cones** e.g. :

- positive orthant : $\mathcal{K}^j = \mathbb{R}^{n+} = \{\boldsymbol{x} \text{ s.t. } x_i \geq 0\} \Rightarrow$ LP
- Lorentz second-order ("ice-cream") cone :

$$\mathcal{K}^j = \{\boldsymbol{x} = (x_0, \bar{\boldsymbol{x}}) \in \mathbb{R} \times \mathbb{R}^{n-1} \text{ s.t. } \|\bar{\boldsymbol{x}}\| \leq x_0\} \Rightarrow \text{SOCP}$$

- cone of positive semi-definite matrix $\boldsymbol{X} \succeq 0 \Rightarrow$ SDP

Linear and conic programming

Linear Programming :

$$\begin{aligned} \max \quad & \boldsymbol{c}^T \boldsymbol{x} \\ \text{s.t.} \quad & \boldsymbol{A}\boldsymbol{x} = \boldsymbol{b} \\ & \boldsymbol{x} \geq 0 \end{aligned}$$

Conic Programming :

$$\begin{aligned} \max \quad & \boldsymbol{c}^T \boldsymbol{x} \\ \text{s.t.} \quad & \boldsymbol{A}\boldsymbol{x} = \boldsymbol{b} \\ & \boldsymbol{x} \in \mathcal{K}^1 \times \ldots \times \mathcal{K}^p \end{aligned}$$

where $\mathcal{K}^j$ are **cones** e.g. :

- positive orthant : $\mathcal{K}^j = \mathbb{R}^{n+} = \{\boldsymbol{x} \text{ s.t. } x_i \geq 0\} \Rightarrow$ LP
- Lorentz second-order ("ice-cream") cone :

$$\mathcal{K}^j = \{\boldsymbol{x} = (x_0, \bar{\boldsymbol{x}}) \in \mathbb{R} \times \mathbb{R}^{n-1} \text{ s.t. } \|\bar{\boldsymbol{x}}\| \leq x_0\} \text{ => SOCP}$$

- cone of positive semi-definite matrix $\boldsymbol{X} \succeq 0$ => SDP
- power cones: $\mathcal{P}_\alpha = \{\mathbf{z} \in \mathbb{R}^m \text{ s.t. } \mathbf{z} = (z_0, z_1, \bar{\mathbf{z}}) \text{ and } z_0^\alpha z_1^{1-\alpha} \geq \|\bar{\mathbf{z}}\|_2, \;\; z_0, z_1 \geq 0\}$

Linear and conic programming

Linear Programming :

$$\begin{aligned} \max \quad & \boldsymbol{c}^T \boldsymbol{x} \\ \text{s.t.} \quad & \boldsymbol{A}\boldsymbol{x} = \boldsymbol{b} \\ & \boldsymbol{x} \geq 0 \end{aligned}$$

Conic Programming :

$$\begin{aligned} \max \quad & \boldsymbol{c}^T \boldsymbol{x} \\ \text{s.t.} \quad & \boldsymbol{A}\boldsymbol{x} = \boldsymbol{b} \\ & \boldsymbol{x} \in \mathcal{K}^1 \times \ldots \times \mathcal{K}^p \end{aligned}$$

where $\mathcal{K}^j$ are **cones** e.g. :

- positive orthant : $\mathcal{K}^j = \mathbb{R}^{n+} = \{\boldsymbol{x} \text{ s.t. } x_i \geq 0\} \Rightarrow$ LP
- Lorentz second-order ("ice-cream") cone :

$$\mathcal{K}^j = \{\boldsymbol{x} = (x_0, \bar{\boldsymbol{x}}) \in \mathbb{R} \times \mathbb{R}^{n-1} \text{ s.t. } \|\bar{\boldsymbol{x}}\| \leq x_0\} \text{ => SOCP}$$

- cone of positive semi-definite matrix $\boldsymbol{X} \succeq 0$ => SDP
- power cones: $\mathcal{P}_\alpha = \{\mathbf{z} \in \mathbb{R}^m \text{ s.t. } \mathbf{z} = (z_0, z_1, \bar{\mathbf{z}}) \text{ and } z_0^\alpha z_1^{1-\alpha} \geq \|\bar{\mathbf{z}}\|_2,\ z_0, z_1 \geq 0\}$

efficient conic programming solvers: CVX, MOSEK, etc.

Conic programming reformulation

Primal variational principle: **smooth** + **non-smooth** term

$$\begin{aligned} \min_{\boldsymbol{u},\boldsymbol{d}} \quad & \int_\Omega \left(\frac{K}{m+1} \|\boldsymbol{d}\|^{m+1} + \sqrt{2}\tau_0 \|\boldsymbol{d}\| \right) \,\mathrm{d}\Omega - \int_\Omega \boldsymbol{f}\cdot\boldsymbol{u}\,\mathrm{d}\Omega \\ \text{s.t.} \quad & \boldsymbol{d} = \tfrac{1}{2}(\nabla \boldsymbol{u} + \nabla^\mathsf{T} \boldsymbol{u}) \\ & \operatorname{div} \boldsymbol{u} = 0 \end{aligned}$$

Conic programming reformulation

Primal variational principle: **smooth** + **non-smooth** term

$$\begin{array}{rl} \displaystyle\min_{\boldsymbol{u},\boldsymbol{d},t} & \displaystyle\int_\Omega \left(\frac{K}{m+1}t^{m+1} + \sqrt{2}\tau_0 t\right) \,\mathrm{d}\Omega - \int_\Omega \boldsymbol{f}\cdot\boldsymbol{u}\,\mathrm{d}\Omega \\ \text{s.t.} & \boldsymbol{d} = \frac{1}{2}(\nabla\boldsymbol{u} + \nabla^\mathsf{T}\boldsymbol{u}) \\ & \operatorname{div}\boldsymbol{u} = 0 \\ & \|\boldsymbol{d}\| \leq t \end{array}$$

Conic programming reformulation

Primal variational principle: **smooth** + **non-smooth** term

$$
\begin{array}{rl}
\displaystyle\min_{\boldsymbol{u},\boldsymbol{d},t,s} & \displaystyle\int_\Omega \left(\frac{K}{m+1}s + \sqrt{2}\tau_0 t\right) \,\mathrm{d}\Omega - \int_\Omega \boldsymbol{f}\cdot\boldsymbol{u}\,\mathrm{d}\Omega \\
\text{s.t.} & \boldsymbol{d} = \frac{1}{2}(\nabla\boldsymbol{u} + \nabla^\mathsf{T}\boldsymbol{u}) \\
& \operatorname{div}\boldsymbol{u} = 0 \\
& \|\boldsymbol{d}\| \leq t \\
& t^{m+1} \leq s
\end{array}
$$

Conic programming reformulation

Primal variational principle: **smooth** + **non-smooth** term

$$\begin{array}{rl}\displaystyle\min_{\boldsymbol{u},\boldsymbol{d},t,s} & \displaystyle\int_\Omega \left(\frac{K}{m+1}s + \sqrt{2}\tau_0 t\right) \,\mathrm{d}\Omega - \int_\Omega \boldsymbol{f}\cdot\boldsymbol{u}\,\mathrm{d}\Omega \\ \text{s.t.} & \boldsymbol{d} = \frac{1}{2}(\nabla \boldsymbol{u} + \nabla^\mathsf{T}\boldsymbol{u}) \\ & \operatorname{div}\boldsymbol{u} = 0 \\ & \|\boldsymbol{d}\| \leq t \\ & t^{m+1} \leq s \end{array}$$

$\Rightarrow$ SOCP/power cone problem in standard format

$$\begin{array}{rl}\displaystyle\min_{\boldsymbol{u},\boldsymbol{x}} & \boldsymbol{c}_u^\mathsf{T}\boldsymbol{u} + \boldsymbol{c}_x^T\boldsymbol{x} \\ \text{s.t.} & \boldsymbol{A}\boldsymbol{u} = 0 \\ & \boldsymbol{B}\boldsymbol{u} - \boldsymbol{x} = 0 \\ & \boldsymbol{x} \in \mathcal{K} \end{array} \quad \rightarrow \quad \begin{Bmatrix} \boldsymbol{A}^\mathsf{T}\boldsymbol{\lambda} - \boldsymbol{B}^\mathsf{T}\boldsymbol{s} + \boldsymbol{c}_u + \boldsymbol{B}^\mathsf{T}\boldsymbol{c}_x \\ \boldsymbol{A}\boldsymbol{u} \\ \boldsymbol{B}\boldsymbol{u} - \boldsymbol{x} \\ \boldsymbol{s}^\mathsf{T}\boldsymbol{x} \end{Bmatrix} = \begin{Bmatrix} 0 \\ 0 \\ 0 \\ 0 \end{Bmatrix}, \boldsymbol{x} \in \mathcal{K}, \boldsymbol{s} \in \mathcal{K}^*$$

Conic programming reformulation

Primal variational principle: **smooth** + **non-smooth** term

$$\begin{array}{ll}\displaystyle\min_{\boldsymbol{u},\boldsymbol{d},t} & \displaystyle\int_\Omega \left(\frac{K}{m+1}s + \sqrt{2}\tau_0 t\right) \,\mathrm{d}\Omega - \int_\Omega \boldsymbol{f}\cdot\boldsymbol{u}\,\mathrm{d}\Omega \\ \text{s.t.} & \boldsymbol{d} = \frac{1}{2}(\nabla\boldsymbol{u} + \nabla^\mathsf{T}\boldsymbol{u}) \\ & \operatorname{div}\boldsymbol{u} = 0 \\ & \|\boldsymbol{d}\| \leq t \\ & t^{m+1} \leq s \end{array}$$

$\Rightarrow$ SOCP/power cone problem in standard format

$$\begin{Bmatrix} \boldsymbol{A}^\mathsf{T}\boldsymbol{\lambda} - \boldsymbol{B}^\mathsf{T}\boldsymbol{s} + \boldsymbol{c}_u + \boldsymbol{B}^\mathsf{T}\boldsymbol{c}_x \\ \boldsymbol{A}\boldsymbol{u} \\ \boldsymbol{B}\boldsymbol{u} - \boldsymbol{x} \\ \boldsymbol{s}^\mathsf{T}\boldsymbol{x} \end{Bmatrix} = \begin{Bmatrix} 0 \\ 0 \\ 0 \\ \mu \end{Bmatrix}$$

$$\boldsymbol{x} \in \mathcal{K}, \boldsymbol{s} \in \mathcal{K}^*$$

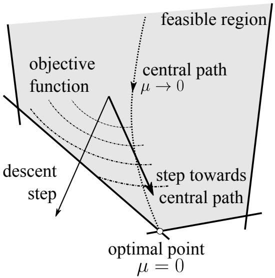

μ defines the **central path**

Lid-driven square cavity

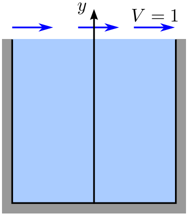

$$Bi = \frac{\tau_0 H}{KV}$$

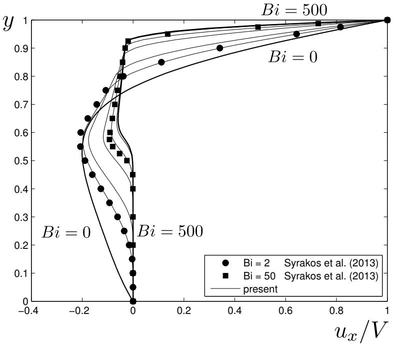

Lid-driven square cavity

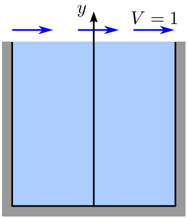

$$Bi = \frac{\tau_0 H}{KV}$$

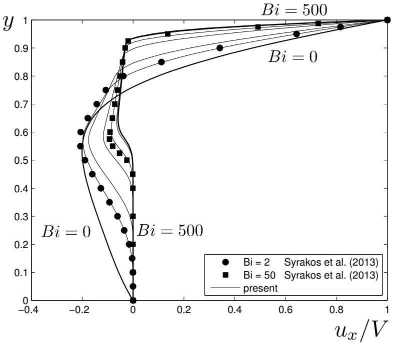

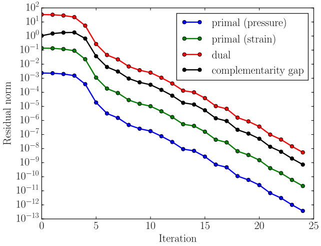

Bi = 2

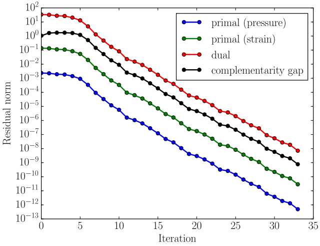

Bi = 200

Lid-driven square cavity

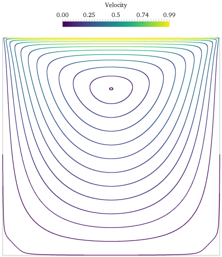

Bi = 0

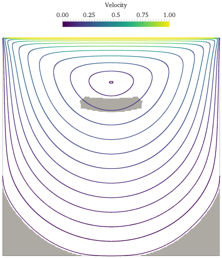

Bi = 1

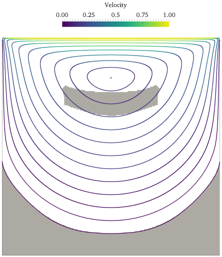

Bi = 2

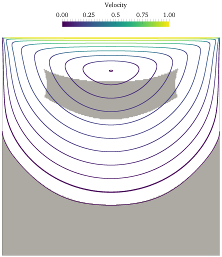

Bi = 5

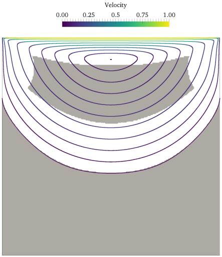

Bi = 20

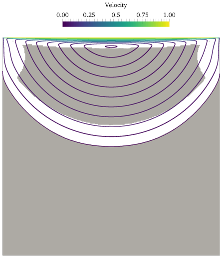

Bi = 200

Eccentric annulus problem

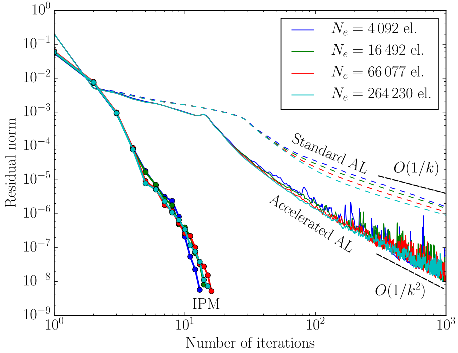

Mesh dependency

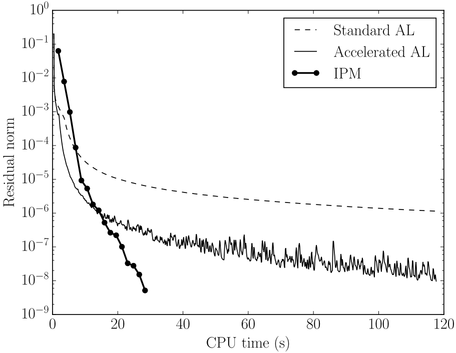

CPU cost ($N_e = 66,077$)

Vane rheometer

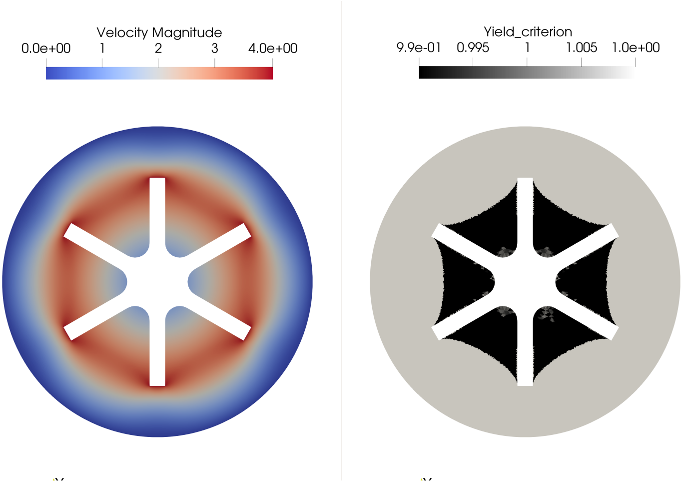

Figure: Bi $= 1$

Vane rheometer

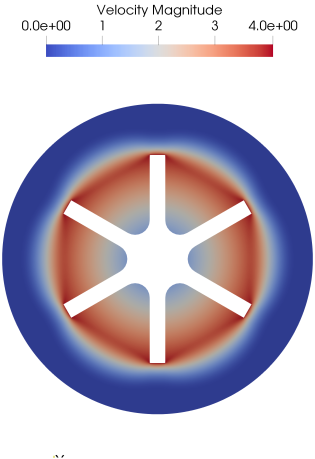

Figure: Bi $= 10$

Vane rheometer

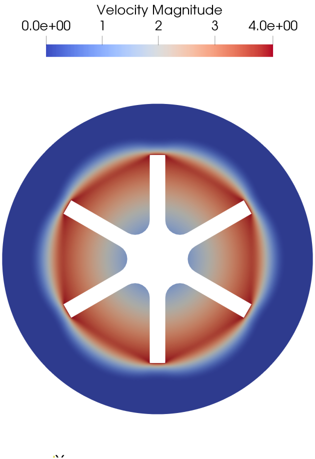

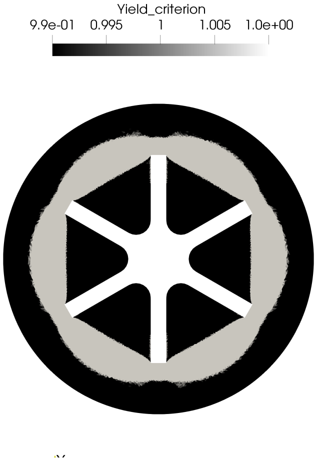

Figure: Bi $= 20$

Vane rheometer

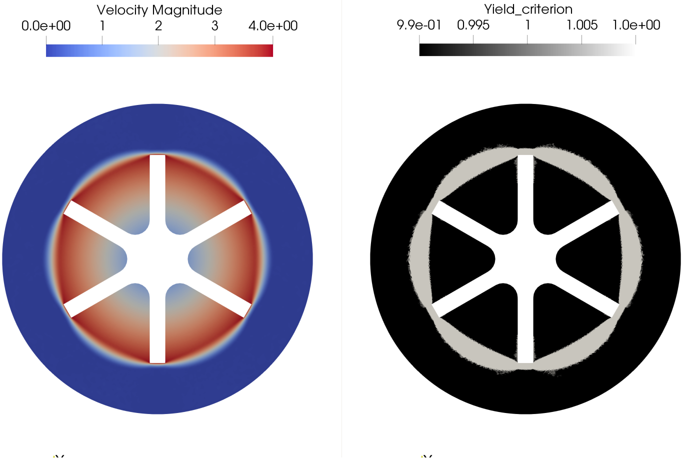

Figure: Bi $= 100$

Flow through a 3D porous medium

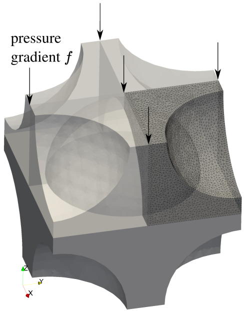

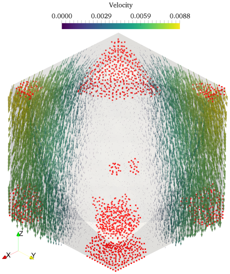

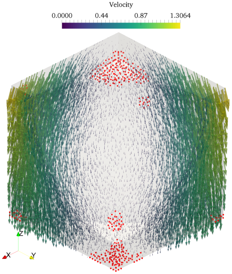

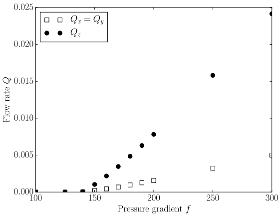

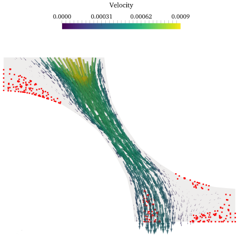

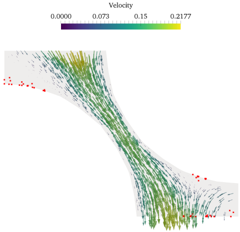

Does it work in practice ?

Extraction of a plate from a viscoplastic fluid bath (Herschel-Bulkley $m = 0.35$)
Fluid velocity field measured by **PIV**

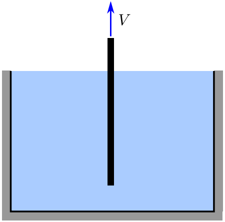

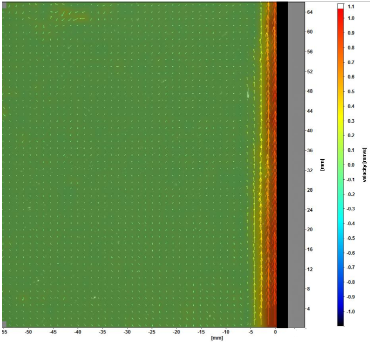

Does it work in practice ?

Extraction of a plate from a viscoplastic fluid bath (Herschel-Bulkley $m = 0.35$)
Fluid velocity field measured by **PIV**

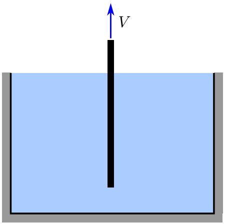

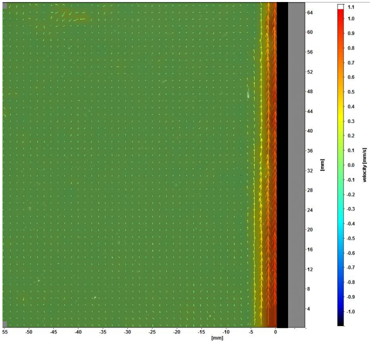

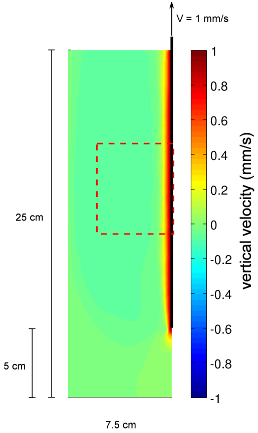

Qualitative comparison :

- velocity profile is uniform in a region away from free surface and plate tip
- fluid is strongly sheared upwards in a small region close to the plate
- moves downwards far from the plate

Extraction of a plate from a yield stress fluid bath

Quantitative comparison of vertical velocity profiles in the uniform region

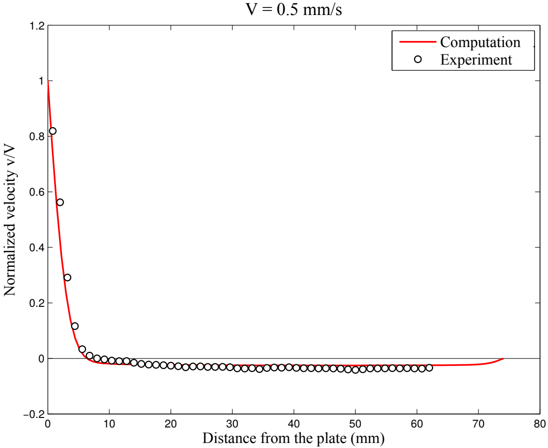

$$V = 0.5\text{mm}/\text{s}$$

Extraction of a plate from a yield stress fluid bath

Quantitative comparison of vertical velocity profiles in the uniform region

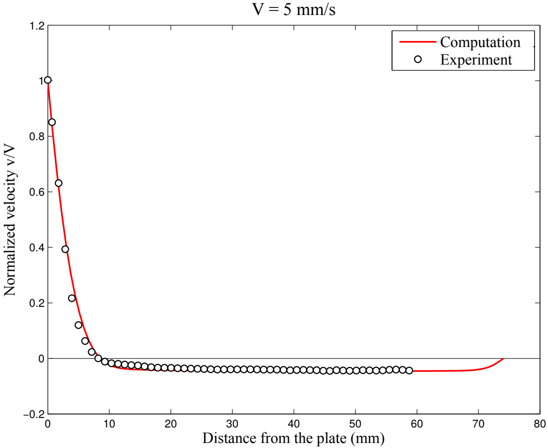

$V = 5\text{mm/s}$

Extraction of a plate from a yield stress fluid bath

Quantitative comparison of vertical velocity profiles in the uniform region

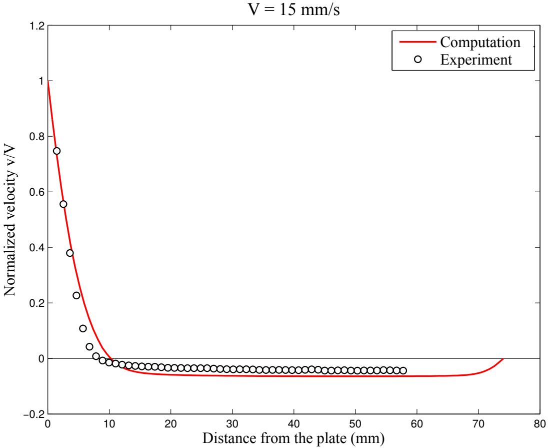

$V = 15\text{mm/s}$

Flow through an expansion-contraction channel

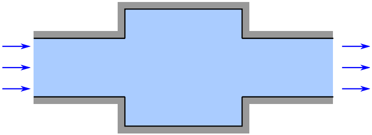

Axial velocity contours

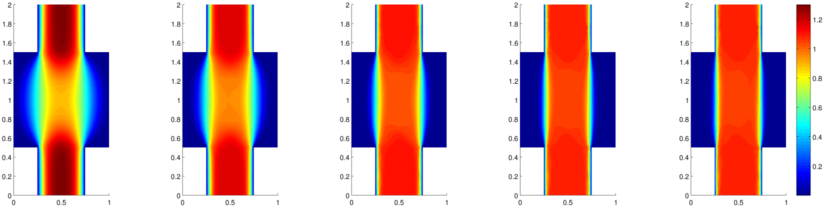

$Bi = 0$ $Bi = 2$ $Bi = 10$ $Bi = 50$ $Bi = \infty$

Flow through an expansion-contraction channel

Axial velocity contours

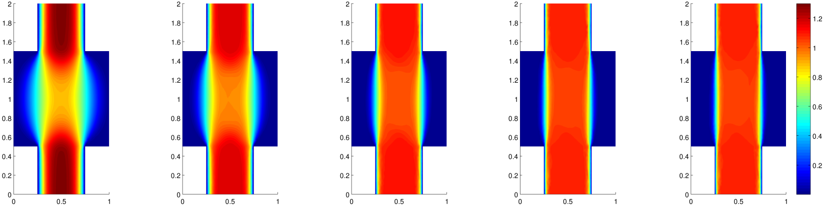

$Bi = 0$ $Bi = 2$ $Bi = 10$ $Bi = 50$ $Bi = \infty$

Velocity fields similar to experimental results of [Chevalier et al., 2013]
flow through a **model pore** with MRI

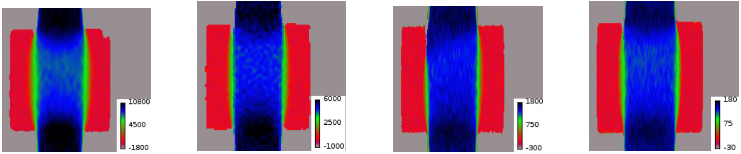

$Bi = 7.0$ $Bi = 8.9$ $Bi = 14.5$ $Bi = 36$

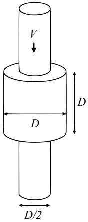

Outline

Rigid particles, bubbles, multiphase

Finite-time settlement of a rigid particle [Wachs and Frigaard, 2016]

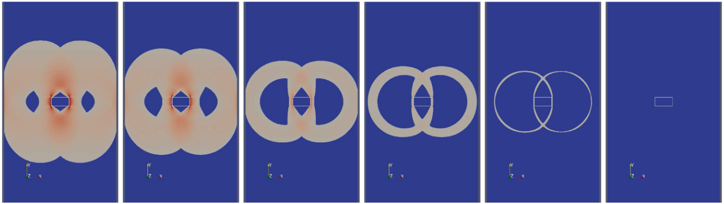

$t/\mathrm{Re} = 0.075$ $t/\mathrm{Re} = 0.125$ $t/\mathrm{Re} = 0.250$ $t/\mathrm{Re} = 0.312$ $t/\mathrm{Re} = 0.337$ $t/\mathrm{Re} = 0.350$

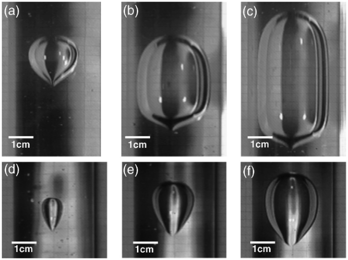

Bubble rise [Dubash and Frigaard, 2007]

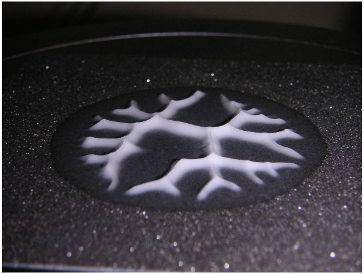

Saffman-Taylor instability [Coussot, Navier]

Submarine landslides, coll. with Xue Zhang (Liverpool)

Some clays, especially **submarine clays** are sensitive to **soil liquefaction**: **strain-softening** viscoplastic behaviour

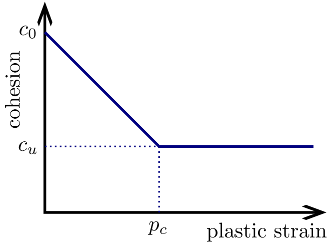

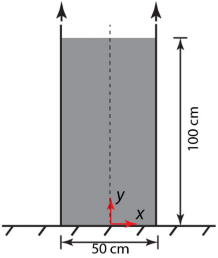

Submarine landslides, coll. with Xue Zhang (Liverpool)

Some clays, especially **submarine clays** are sensitive to **soil liquefaction**: **strain-softening** viscoplastic behaviour

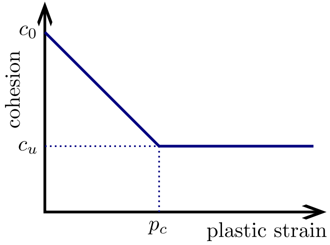

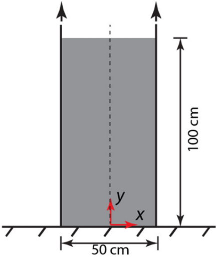

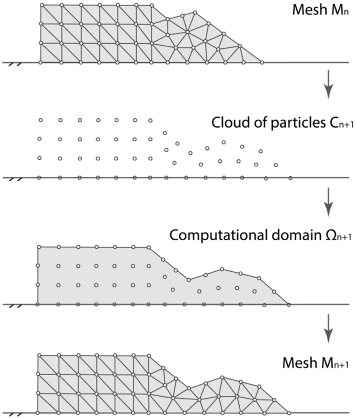

Particle Finite-Element Method

Submarine landslides, coll. with Xue Zhang (Liverpool)

Column collapse

[ ]pdfmark=/ANN, /F (SensitiveColumnCollapse.mp4) /Poster true »,Annotations=« /Mode /Repeat »,T=(mmdefaultlabel2), Border=0 0 0

Submarine landslides, coll. with Xue Zhang (Liverpool)

Slope collapse

[ ]pdfmark=/ANN, /F (SensitiveSlopeCollapse.mp4) /Poster true »,Annotations=« /Mode /Repeat »,T=(mmdefaultlabel5), Border=0 0 0

Submarine landslides, coll. with Xue Zhang (Liverpool)

Slope collapse

[ ]pdfmark=/ANN, /F (SensitiveSlopeCollapse.mp4) /Poster true »,Annotations=« /Mode /Repeat »,T=(mmdefaultlabel7), Border=0 0 0

retrogressive failure

Conclusions and Outlook

Conclusions

- **yield stress fluid flows** are challenging to solve due to **unknown rigid regions**
- **simple regularization fails** to accurately capture rigid region locations
- **conic programming methods** are well suited to handle **non-smoothness**

Outlook

- efficient numerical methods still need for **multiphase flows**
- adaptation to **shallow water equations** (avalanches)
- inclusion of **elasticity**

Conclusions and Outlook

Conclusions

- **yield stress fluid flows** are challenging to solve due to **unknown rigid regions**
- **simple regularization fails** to accurately capture rigid region locations
- **conic programming methods** are well suited to handle **non-smoothness**

Outlook

- efficient numerical methods still need for **multiphase flows**
- adaptation to **shallow water equations** (avalanches)
- inclusion of **elasticity**

Thank you for your attention !